

**Avco**  
CORPORATION

**defense and industrial products group**

Spaceflight Programs Office • 6501 East Admiral Place  
Drawer N — Admiral Station • Tulsa 15, Oklahoma • TEmple 5-6911

FILE  
RADIATION

2092/3

September 27, 1963

**N 65-35 107**

FACILITY FORM 802

(ACCESSION NUMBER)

31

(PAGES)

CR 4239

(NASA CR OR TMX OR AD NUMBER)

(THRU)

(CODE)

64

(CATEGORY)

Dr. Frank B. Voris  
Chief of Human Research  
Biotechnology and Human Research  
Office of Advanced Research and Technology  
National Aeronautics and Space Administration  
Washington 25, D. C.

Dear Dr. Voris:

The Avco Spaceflight Programs Office is pleased to submit the First Quarterly Report on contract NASw-782 entitled "Study of Correlation Between Linear Energy Transfer and Relative Biological Effectiveness." As is indicated, the progress to date has been exceptionally rewarding and we are looking forward to a presentation at NASA Headquarters at your earliest convenience. Program expenditures to date are within our initial projections, and in every other respect, the project is on schedule.

GPO PRICE \$ \_\_\_\_\_

CFSTI PRICE(S) \$ \_\_\_\_\_

Hard copy (HC) 2.00

Microfiche (MF) .50

ff 653 July 65

Very truly yours,

AVCO CORPORATION  
SPACEFLIGHT PROGRAMS OFFICE

*H. V. Stewart*

H. V. Stewart, Manager  
Space Environment Programs

HVS:mbw

STUDY OF THE CORRELATION BETWEEN  
LINEAR ENERGY TRANSFER AND  
RELATIVE BIOLOGICAL EFFECTIVENESS

Prepared by

Avco/Spaceflight Programs Office  
Tulsa, Oklahoma  
and  
Oklahoma University Research Institute  
Norman, Oklahoma

Contract NASw-782  
1 July 1963 - 1 October 1963

Prepared for

National Aeronautics and Space Administration  
Washington, D. C.

## I. INTRODUCTION

In compliance with terms of the subject contract, hereby submitted is the first of four quarterly progress reports. Work is continuing on phase one as outlined in the original proposal (section II. B., p. 2); and, except for minor variations, the methods described in the proposal are unaltered.

## II. PROCEDURE AND RESULTS

The course of action on this experiment is to instrument the physical parameters, LET and absorbed dose, and observe the lethal effect upon a living biological system (in this case, yeast). The experimental procedure is to first establish an RBE of one for the biological system with 200 KVCP x-rays; quantitate the absorbed dose using a Tissue Equivalent Ionization Chamber (TEIC); and, then, holding dose constant, vary and measure the LET by changing types of radiation and their incident energies. In this manner, two contributing factors to cell death are measured and the amount of killing is observed through the decrease in the biological system's viability.

To perform this experiment, three parameters must be known, rad dose, LET, and cell viability, where each is to be fixed within limits of the stated case. To establish cell viability, yeast in a compacted mass are irradiated, then the cell mass is sectioned at various depths, and plate counts are made of each section. To establish LET, an instrument is designed that measures, within the dimensions of a single cell, transfer of energy to the surrounding medium by an ionizing particle. To establish dose, an instrument is designed that measures absorbed dose at a macroscopic point within a medium in units of ergs/gm.

Results of experiments with a compacted yeast cell mass have indicated that, with adequate control, this technique is successful. A pedigreed and, therefore, genetically homogeneous strain of yeast is suspended in a gelatinous solution and compacted by a centrifuge into a uniform diameter cavity within a wax container. After jelling, the

cell packet is subjected to radiation experimentation. Following irradiation, ten micron slices are removed consecutively from the cell mass and compared to equal thicknesses of unirradiated control sectioned at the same depth. The resulting difference in plate counts of the two sections is attributed to cell death by radiation.

Results of an analysis of the spectrum of pulses to be obtained from the LET sensor show that the LET spectrum,  $D(L)$ , is related to the pulse height spectrum,  $N(h)$ , through the relationship:

$$D(L) = K_1 h^2 \frac{d}{dh} \left[ \frac{N(h)}{h} \right]$$

In addition, the absorbed dose,  $Q_{rad}$ , can be obtained from the pulse height spectrum through the relationship:

$$Q_{rad} = K_2 \left\{ \left[ h^2 N(h) \right]_0^{h_{max}} - 3 \int_0^{h_{max}} h N(h) dh \right\}$$

The latter furnishes a numerical value of the same parameter,  $Q_{rad}$ , through two methods of measurement--the LET sensor and the dose rate sensor.

The dose rate measuring instrument is a Bragg-Gray ionization chamber which has cavity walls constructed of a tissue equivalent plastic and the cavity itself is filled with a matching gas. Since the ratio of relative mass stopping powers of wall to gas is unity, the energy dissipated in the cavity becomes

$$E = WJ$$

where  $W$  is the energy required to produce an ion pair in the gas and  $J$  is the ion pairs formed in the gas per gram per second as measured by the current produced in the cavity.

### III. CONCLUSIONS AND RECOMMENDATIONS

The biological aspect of this experiment will require considerable effort to make the experimental procedure one in which no loss of data will result from accidentally losing a sectioned piece of cell mass. The gelatinous suspension of cells must be hardened by freezing in order for it to be sectioned. Even with extreme care, loss of data results because the cell mass will either push away from the microtome blade if not cold enough or shatter if too cold.

Gelatin is desired for the suspending medium, not only because it is proteinaceous and, therefore, has similar radiation absorption qualities as muscle tissue, but because it allows for yeast cells to be irradiated in a wet state. The latter quality affords a more radiation sensitive biological system while the former presents radiation scattering cross sections similar to those of living tissue. For these reasons gelatin suspension is to be maintained, and two methods of solution to the sectioning problem are being pursued: One, make a gelatin that is rigid enough to section at room temperature, two, obtain better control over the freezing process. There is no progress to report on method one; and with method two, a new microtome has been ordered which sections the cell mass with a horizontal rather than a vertical motion. With this tool, better control over the freezing process can be maintained.

During the next report period, the sectioning problem will be surmounted, and experiments will be in progress to establish an RBE of one for the biological system. Also, assembly of the LET sensing unit will be completed, and data will be obtained from a primary calibration of the device.

Primary calibration will be obtained by placing a mono-energetic alpha source on the end of a 1/16 inch diameter rod. The source will be positioned at measured distances along a radius from the center of the spherical cavity. With the source positioned at the cavity wall, a unique pulse height distribution will emanate (see Appendix A). As the source is positioned away from the cavity the

particles will become collimated along a major diameter and another distribution of pulse heights will be observed. Finally, when the source distance becomes great enough, gas absorption will slow the particles until maximum transfer of energy to the medium results, and the so-called Bragg Peak will be observed.

Assembly and calibration of the ionization chamber will be completed during the next report period. Since this device is designed to measure absorbed dose in tissue, variations to response as a function of wavelength need not be considered. Consequently, calibration over the entire dynamic range can be obtained by establishing a point on the transfer curve (absorbed dose vs. output voltage) with a known  $\text{Co}^{60}$  activity at a measured distance from the cavity center. By matching this output with a fixed intensity and beam quality from an x-ray machine at a particular source-sensor distance, calibration can be completed via the inverse square law.

The ionization chamber will provide data in units of rad per hour in tissue, but rad in tissue is desired. Temporarily, integration of the dose rate vs. time data can be performed by multiplication of the coordinates; but, if in the future instability of the radiation sources is experienced (neutrons and protons), it is recommended that an electronic means of integration be devised.

#### IV. DATA AND INFORMATION

##### A. Biological

A compacted mass of yeast cells to serve as a tool for evaluating tissue radiation damage as described in the original proposal is retained, with the following modifications:

1. Experimental results have shown that the commercial yeast source (Red Star Brand Dried Yeast), though seemingly advantageous because of availability, viability, and lack of microbial contamination, has too much physiological variability from batch to batch; thus the radiation response is not predictable.

Therefore, this source has been abandoned in favor of more reliable Sc-6 diploid and Sc-7 haploid pedigreed strains of yeast. For present studies, Sc-7 strain has been grown in 20 liter carboys, harvested, washed five times in sterile 0.85 percent saline and stored in the refrigerator until used. Studies on cells so treated have been reproducible.

2. Experiments have been performed which were designed to evaluate the effect of radiation damage over varying degrees of cell dilutions. These data indicate there is little or no effect on the percent survival after x-ray treatment for dilutions from 1 gram wet cells per 5 ml diluent through 1 gram wet cells per 2 liters diluent. Some very recent experiments have indicated that, as the concentration of yeast cells approaches a paste, there is a difference in response to x-ray damage, and such experiments are being continued.
3. Since an irradiated mass of yeast cells studied in toto cannot yield quantitative information about the effect of a Bragg Peak occurring within the cell mass, it is desirable to account for cell damage in small, regular increments from the

nearest to the most distant cells with respect to the radiation source. To accomplish this a number of variations of a basic approach have been attempted.

a. Approach #1

Laminated plastic wafers containing a monolayer of yeast cells are pressed into a mass of cell sandwiches. The layers of plastic are necessary to keep the yeast layers retrievable. Aside from the obvious difficulty of preparing such sandwiches, the relative thickness of the plastic wafers presents a problem; and if there is to be continuity of fluids from one layer to another, the technique is limited to the use of porous materials such as bacteriological plastic filters. Unfortunately, such plastic filters are usually in excess of 100 microns in width.

To test reproducibility with this technique, four wafers were prepared, pressed together, then separated and placed into 10 ml of diluent. After vigorous agitation plate counts from 1 ml samples ranged from 161 to 179 colonies.

b. Approach #2

The yeast cells are embedded in a 20 percent gelatin solution, centrifuged to pack the cells so that the gelatin acts as a cementing substance holding the mass of cells together, then after cooling the gel, 10 micron slices are obtained with a microtome and each slice plated to determine the viable count for that respective 10 micron section. In this way, the Bragg Peak can be located and studied. Some advantages favoring the use of gelatin for embedding are its radiation absorption characteristic, its compatibility with living yeast cells, and prevention of movement of cells within the mass. Furthermore,

bacteriological gelatin melts at less than 45°C which allows easy recovery of the cells from the section by heating the diluent to which has been added the 10 micron section. It has been shown that the microtome knife destroys a relatively constant number of cells on each pass through the cell mass. Work to date has centered on refinement of techniques to gain the greatest possible precision.

Various embedding techniques have been attempted including cell-gelatin mass in tygon tubing, cell-gelatin mass surrounded by paraffin, sodium stearate-cell mass, cells and gums such as arabic, synthetic gums (B. F. Goodrich) and gels such as agar and pectin.

The most promising results have been obtained with frozen suspensions of cells in gelatin surrounded by paraffin.

Results of two separate experiments are tabulated in Table I with a plot of the first experiment indicated by Figure 1.

#### B. LET Sensor

A methane filled gas-flow proportional counter has been designed, and a working prototype model of it has been fabricated from lucite. (Final design will be constructed of tissue equivalent plastic.) Figure 2 is a cross sectioned drawing of the device. The sensitive volume is a 0.5 inch diameter sphere with a 0.001 inch platinum anode placed along a diameter.

The electric field distribution within the cavity produced by this geometry deviates from the ideal (a radial field inversely proportional to the radial distance from the anode) as indicated by the field distribution plot in Figure 3. Since multiplication does not occur at regions other than the high field in the immediate vicinity of the anode, and since the

TABLE I

Measurement of Depth Dose

200 KV x-ray/Dose 20,000 r		Unirradiated Control	
Consecutive 10 Micron Sections	Average Plate Count	Consecutive 10 Micron Sections	Average Plate Count
1	24	1	350
2	49.6	2	360
3	62	3	320
4		4	350
5	113	5	360
6	143.8	6	
Second Experiment			
1		1	$10.7 \times 10^3$
2		2	$11.4 \times 10^3$
3	115	3	$11.8 \times 10^3$
4	119		
5	116		
6	139		
7	152		

K&E 10X10 TO THE CM. 359-14  
KEUFFEL & ESSER CO. MADE IN U.S.A.

AVERAGE COLONIES

600  
500  
400  
300  
200

UNIRRADIATED  
CONTROL  
(SC-7 YEAST)

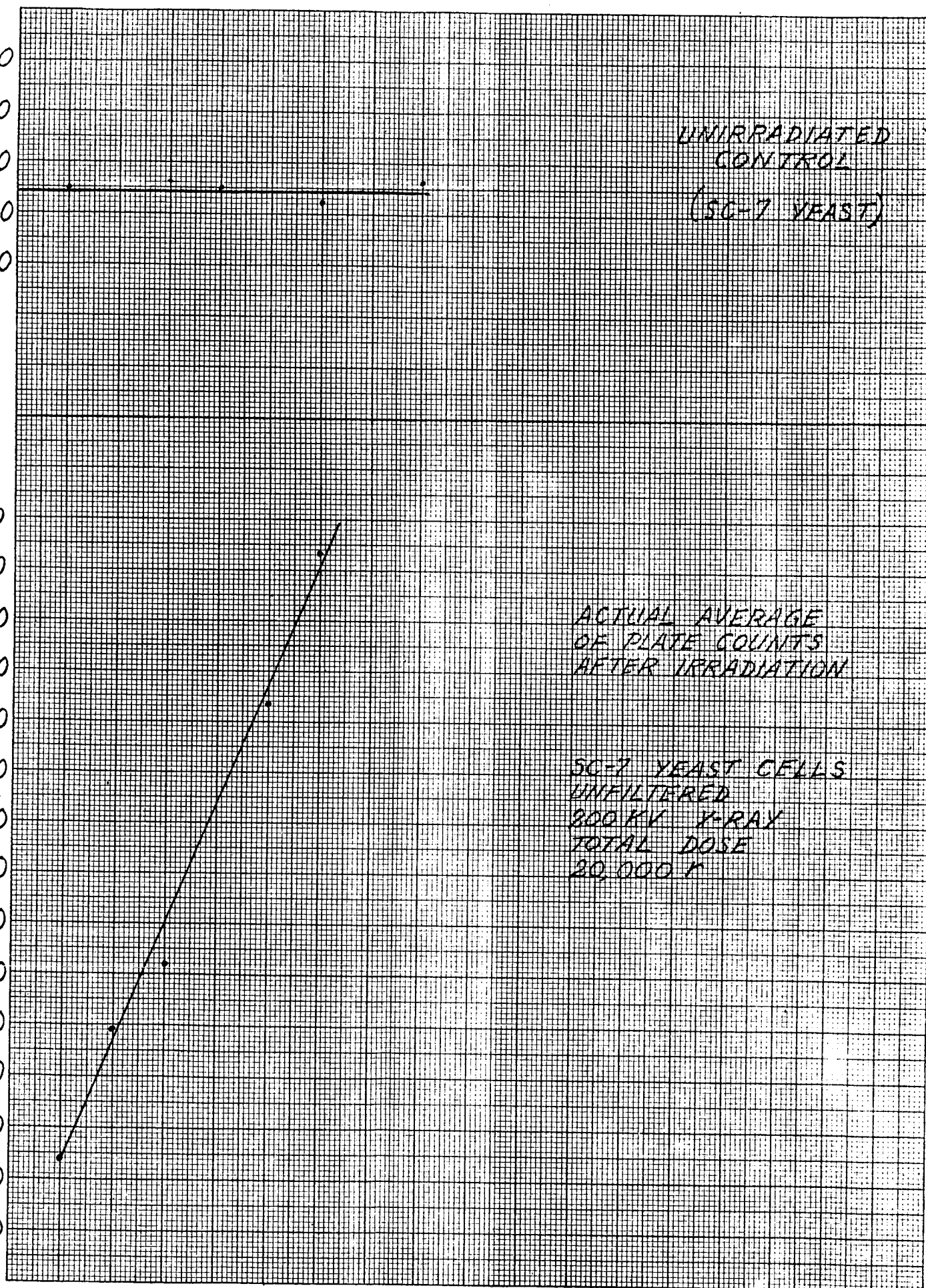
50  
40  
30  
20  
10  
100  
90  
80  
70  
60  
50  
40  
30  
20  
10

ACTUAL AVERAGE  
OF PLATE COUNTS  
AFTER IRRADIATION

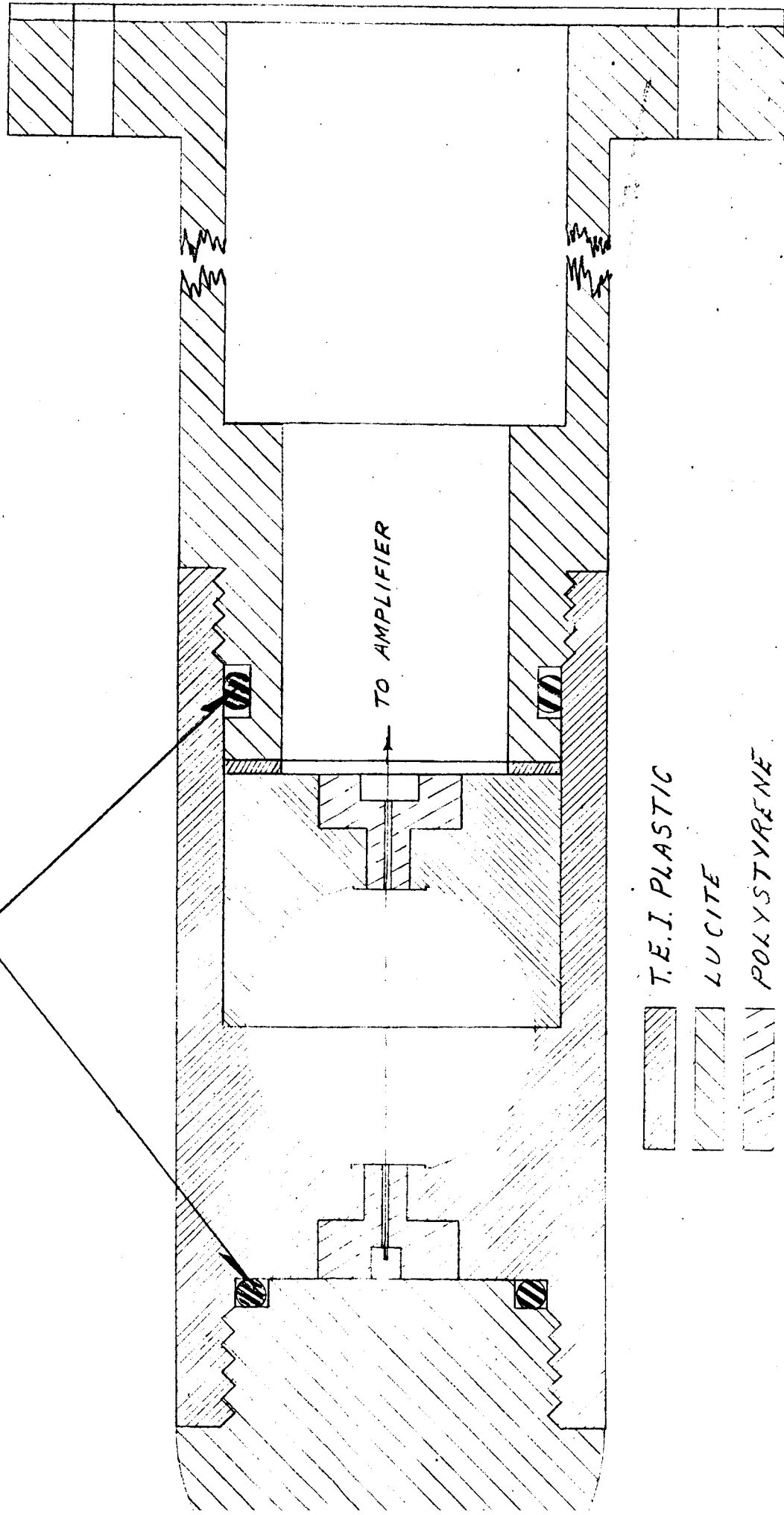
SC-7 YEAST CELLS  
UNFILTERED  
200 KV X-RAY  
TOTAL DOSE  
20,000 R

10 20 30 40 50 60 70  
DEPTH IN CELL MASS (MICRONS)

FIG. 1



"O" RING SEALS



T.E.I. PLASTIC

LUCITE

POLYSTYRENE

NICKEL

FIG. 2 - CROSS SECTION OF LET SENSOR

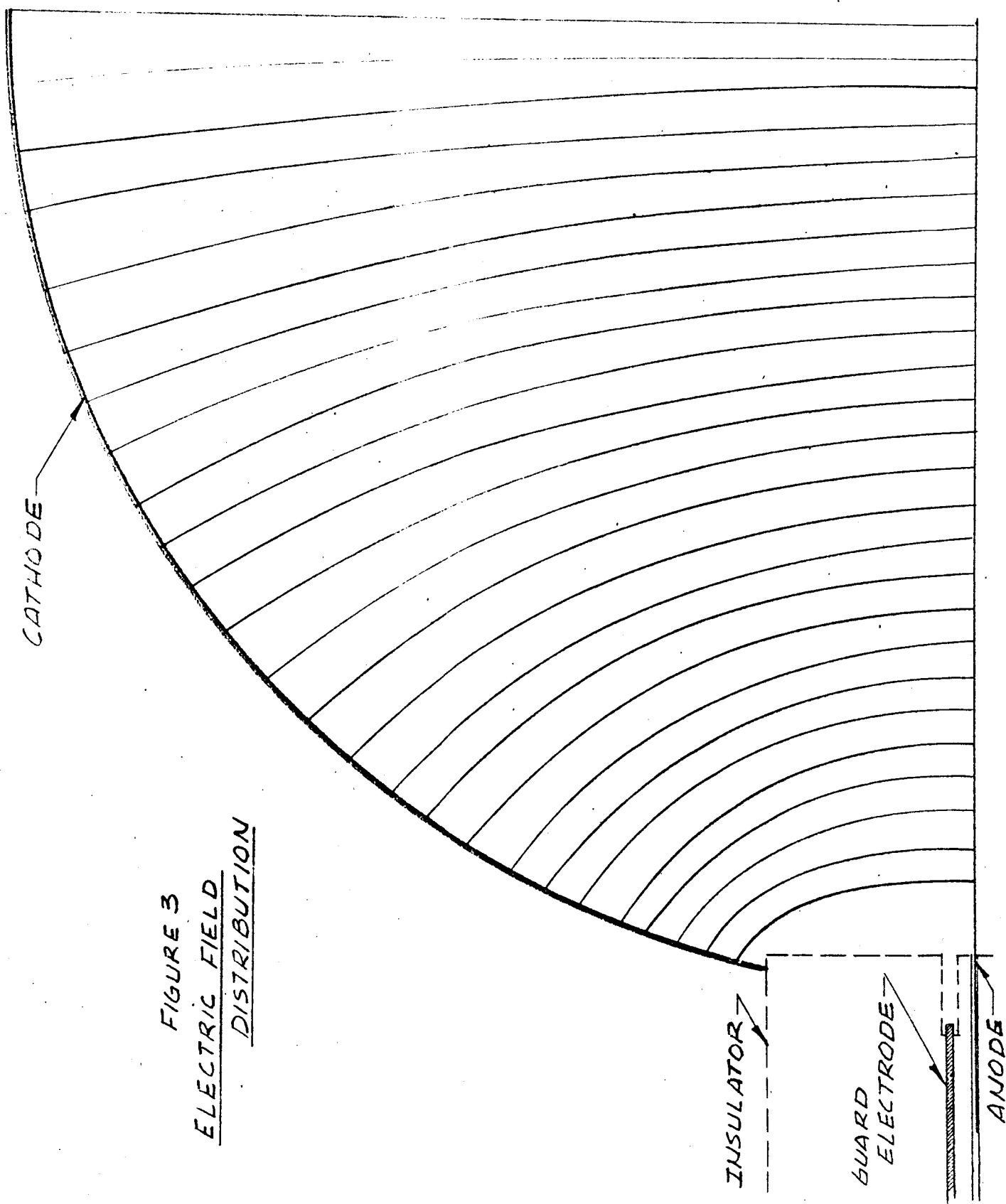


**FIGURE 3**  
**ELECTRIC FIELD**  
**DISTRIBUTION**

high field region in this case is essentially radial, uniform multiplication should result over the total length of the anode. Proof of this, however, awaits experimentation.

The data in Figure 3 represent field lines corresponding to a cathode having a cylindrical geometry with the anode across a diameter. These data were obtained by applying 50 volts potential across conducting paper having silver paint electrodes. The dimensions indicated are actual.

Other work performed on the LET sensor includes an analysis of the data to be obtained from it. During radiation experimentation, the LET sensing device will produce a spectrum of the number of counts per channel vs. pulse height, and an analytical interpretation of the pulse height spectrum is required.

The designed sensor operates on the principle of a proportional counter, and it is not difficult to show that the distribution of the number of electrons collected,  $N(E)$ , equals the product of  $n$ , the number of gas atoms per unit volume in the sensor cavity;  $A$ , the gas multiplication constant;  $\sigma(E)$ , the gas ionization cross section; and  $P(\lambda)$ , the path length distribution of the ionizing particles through the cavity or

$$N(E) = nA\sigma(E)P(\lambda)$$

Since energy lost by the ionizing particle as it traverses the sensor cavity is negligible compared to the incident energy,  $\sigma(E)$  can be considered constant, which leaves  $P(\lambda)$ , the path length distribution, to be evaluated (Appendix A).

$P(\lambda)$  depends upon where the source is located with respect to the sensor cavity. In the case of an omnidirectional flux,  $P(\lambda) = \lambda/2R^2$  where  $R$  is the cavity radius.

The pulse height amplitude,  $h$ , generated in the cavity is a linear function of the number of electrons

collected; and, when the LET sensor is exposed to radiation, a spectrum  $N(h)$ , which represents the number of pulses per pulse-height interval at various pulse-height intervals, is measured. This function is related to the LET spectrum,  $D(L)$ , of the ionizing particles by

$$N(h) = K_1 h \int_{\frac{\alpha h}{2R}}^{\infty} \frac{D(L)}{L^2} dL$$

where  $\alpha$  is a constant relating the energy deposited in the chamber to the pulse height. From the pulse height spectrum, the LET spectrum is found by differentiating to produce (Appendix B)

$$D(L) = K_2 h^2 \frac{d}{dh} \left[ \frac{N(h)}{h} \right]$$

Also, the absorbed dose can be obtained from  $N(h)$  (Appendix C).

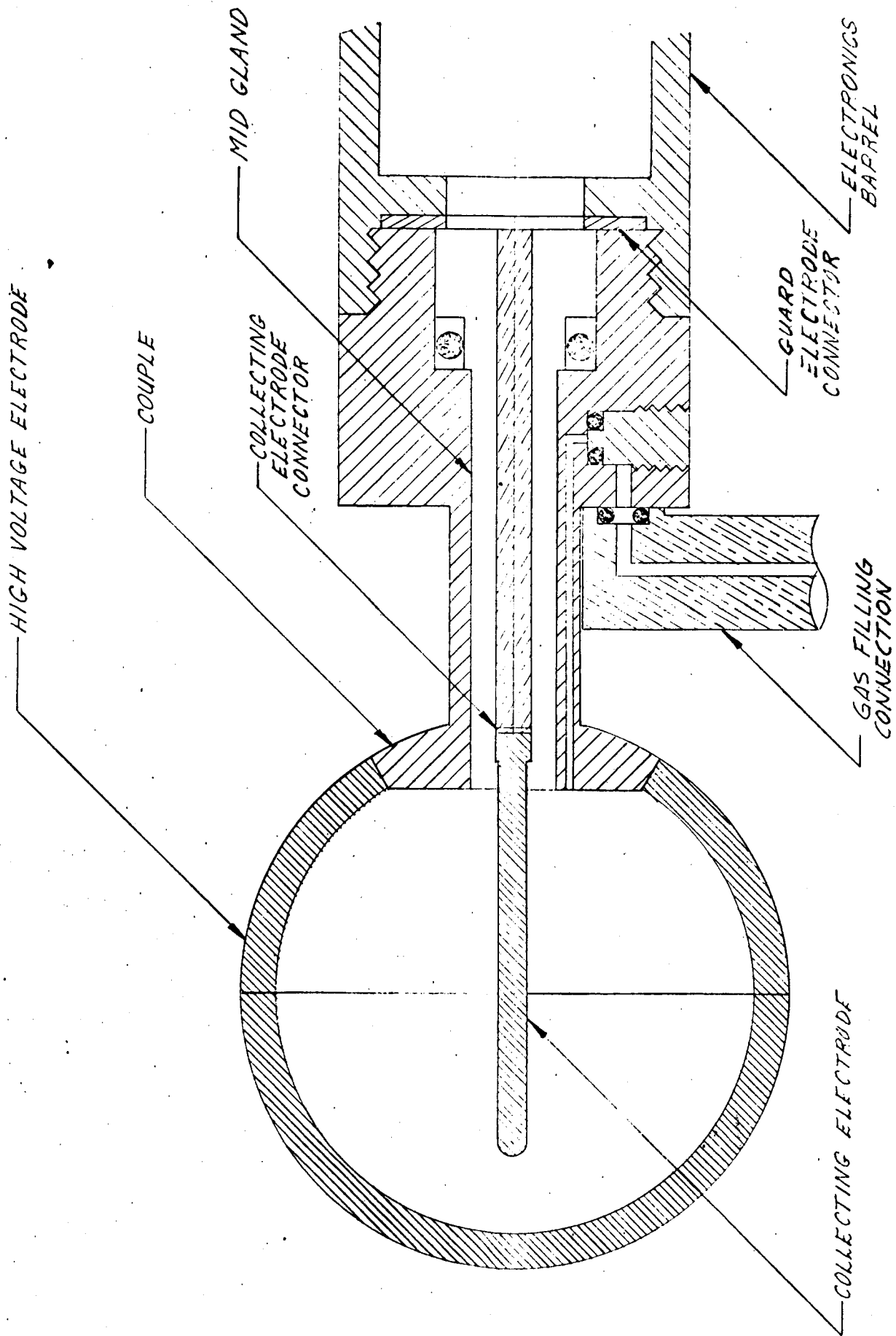
$$Q_{\text{rad}} = K_3 \left\{ \left[ h^2 N(h) \right]_0^{h_{\text{max}}} - 3 \int_0^{h_{\text{max}}} h N(h) dh \right\}$$

The latter equation affords an opportunity to cross check values from the LET measuring instrument with the dose measuring instrument.

### C. Dose Sensor

An instrumentation system is designed to measure the absorbed dose in tissue from all ionizing radiations. The sensing element of the instrument is a tissue equivalent ionization chamber designed to conform to the Bragg-Gray principle (see Figure 4).

The most convenient method for measurement of radiation energy absorbed by a given material is through the use of the Bragg-Gray relation. Derivation of this relation and the basic conditions



SCALE 4:1

FIG. 4 ASSEMBLY

necessary for its use are presented in Appendix D. The cavity ionization principle permits a determination of energy absorption in a solid medium from the measured ionization in a small gas-filled cavity. This principle is the basis for the energy deposition dosimetry to be used in these experiments.

The design of the chamber cavity was influenced by the desire to achieve high sensitivity, good ion collection, and to minimize the problems associated with data reduction and interpretation.

Since a tissue equivalent filling gas will be employed, the dimensions of the cavity can be larger than for an air filling. Consequently, the cavity volume has been designed such that it is large enough for suitable radiation sensitivity and small enough to be compatible with the LET sensor. The electronic system to be used employs a sensitive electrometer tube with a grid current operating range between  $10^{-14}$  and  $10^{-5}$  amps. A cavity volume of 5 cc will yield a current of  $4.7 \times 10^{-14}$  amps at the desired minimum dose rate of 0.10 rads per hour.

To minimize the problems associated with data reduction and interpretation, this volume is achieved with a spherical cavity that has uniform directional sensitivity.

A conducting plastic is used for the cavity walls which reproduces tissue absorption coefficients as recommended by the International Commission of Radiological Units within small errors. This plastic has the following chemical formulation:

C<sub>1.024</sub> H<sub>10.2</sub> O<sub>4.556</sub> N<sub>0.25</sub> Na<sub>0.0035</sub> Mg<sub>0.0008</sub>  
P<sub>0.0065</sub> Si<sub>0.0756</sub> K<sub>0.0077</sub> Ca<sub>0.00017</sub>

In addition to being a tissue equivalent medium, the plastic is rigid, durable, can be compression-moulded, has adequate electrical conductivity, and is impervious to and free from chemical attack by the filling gas.

The cavity wall thickness will be 0.0625 inch to increase the usefulness of the instrument for measuring dose rates due to ionizing radiations with low penetrating power.

Table II is a tabulation of other tissue equivalent materials surveyed along with their chemical formulations indicated as percentages by weight.

Since the ionization chamber is to be used for measuring rads in a tissue equivalent medium, both the chamber wall and gas are matched to the medium. A suitable nonexplosive tissue equivalent gas is a mixture of methane, carbon dioxide, and nitrogen with a percent by weight composition of:

C	-	45.6
O <sub>2</sub>	-	40.8
H <sub>2</sub>	-	10.1
N <sub>2</sub>	-	3.5

Observations of the gamma and neutron sensitivity of a tissue equivalent ionization chamber using this filling gas have indicated a stability within the measuring accuracy of  $\pm 2\%$  over a period of more than six months, thus indicating that no measurable change in the filling gas has occurred through diffusion or adsorption losses in the cavity wall during this time.

The configuration of the collecting electrode is important for proper operation of the ionization chamber. Its geometry determines the collection efficiency as well as the response time (capacity) of the instrument. The diameter for the collecting electrode of this chamber (0.050 in.) is large enough for good structural integrity and high collection efficiency, but small enough to maintain low capacity.

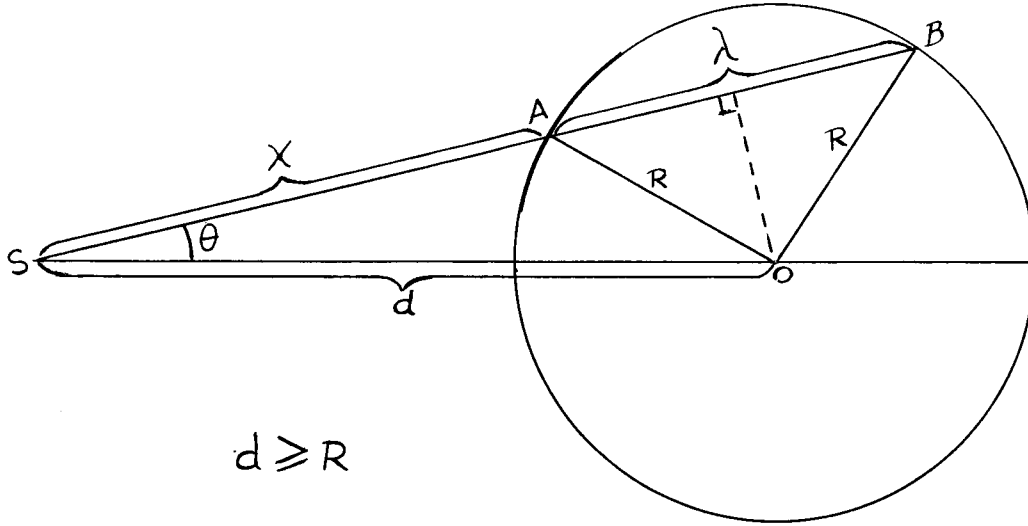
TABLE II

Compositions of Various Tissue Equivalent Plastics and Gases

Element	Alderson (% by weight)	Shonka (% by weight)	Markite (% by weight)	Polyethylene (% by weight)	Tissue Equiva- lent Gas (% by weight)
Carbon	64.803	12.3	86.4	86.5	45.6
Hydrogen	8.891	10.2	5.6	10	10.1
Oxygen	22.181	73.0	4.3		40.8
Nitrogen	3.150	3.5	3.7	3.5	3.5
Magnesium	0.034	0.02			
Iron	0.005				
Sulfur	0.280	0.2			
Potassium	0.172	0.5			
Sodium	0.094	0.05			
Phosphorus	0.268	0.2			
Chlorine	0.122				
Calcium		0.03			

## APPENDIX A

### Calculation for Path-Length Distribution of Particles through a Spherical Cavity



It is desired to find the probability distribution function,  $P(\lambda)$ , for the path-length  $\lambda$ .

If  $\Omega_0$  is the total solid angle subtended by the sphere at the source S, then  $P(\lambda) d\lambda = P(\Omega) d\Omega = -2\pi/\Omega_0 \sin \theta d\theta$ , is the probability for the path length to lie between  $\lambda$  and  $\lambda + d\lambda$ , corresponding to a solid angle between  $\Omega$  and  $\Omega + d\Omega$ .

The problem, therefore, reduces to the evaluation of  $\frac{\sin \theta d\theta}{\Omega_0}$  as a function of  $\lambda$ ,  $d$ ,  $R$ , and  $d\lambda$ .

$$(1) \quad d \cos \theta = x + \frac{\lambda}{2}$$

In the triangle SOA, by the cosine rule, we have,

$$(2) \quad \cos \theta = \frac{x^2 + d^2 - R^2}{2xd}$$

Substitution for  $\cos \theta$  in (1) produces,

$$\frac{x^2 + d^2 - R^2}{2x} = x + \frac{\lambda}{2}$$

or  $x^2 + \lambda x - (d^2 - R^2) = 0.$

$$\therefore x = -\frac{\lambda}{2} \pm \sqrt{\frac{\lambda^2}{4} + (d^2 - R^2)}$$

To choose the proper sign,  $d = R$  at  $x = 0$ . Hence the plus sign must be chosen or,

$$(3) \quad x = -\frac{\lambda}{2} + \sqrt{\frac{\lambda^2}{4} + d^2 - R^2}$$

Substituting for  $x$  in (1),

$$d \cos \theta = \left[ \frac{\lambda^2}{4} + (d^2 - R^2) \right]^{1/2}$$

$$\therefore \sin \theta d\theta = \frac{-\lambda d \lambda}{4d \sqrt{\frac{\lambda^2}{4} + (d^2 - R^2)}}$$

$$\begin{aligned} \text{Again, } \Omega_0 &= 2\pi \int_0^{\cos^{-1} \frac{\sqrt{d^2 - R^2}}{d}} \sin \theta d\theta \\ &= 2\pi \left[ 1 - \frac{\sqrt{d^2 - R^2}}{d} \right] \end{aligned}$$

$$\text{Hence } P(\lambda) d\lambda = -\frac{2\pi}{\Omega_0} \sin \theta d\theta$$

$$= 2\pi \frac{\lambda d \lambda}{4d \sqrt{\frac{\lambda^2}{4} + (d^2 - R^2)}} \times \frac{1}{2\pi \left[ 1 - \frac{\sqrt{d^2 - R^2}}{d} \right]}$$

$$(4) \text{ or } P(\lambda) = \frac{\lambda}{4d^2 \sqrt{1 - \frac{R^2}{d^2} + \frac{\lambda^2}{4d^2}} \left( 1 - \sqrt{1 - \frac{R^2}{d^2}} \right)}$$

Now consider the two limiting cases, that is,

Case 1:  $d = R$

$$\text{Then } P(\lambda) = \frac{\lambda}{4R^2 \times \frac{\lambda}{2R} \times 1}$$

$$(5) \quad = \frac{1}{2R}$$

$$\text{And } \langle \lambda \rangle = \int_0^{2R} \lambda P(\lambda) d\lambda = \frac{1}{2R} \int_0^{2R} \lambda d\lambda$$

$$(6) \quad = R$$

Case 2:  $d \longrightarrow \infty$

$$P(\lambda) = \frac{\lambda}{4d^2 \sqrt{1 - \frac{R^2}{d^2} + \frac{\lambda^2}{4d^2}} \left[ 1 - \left( 1 - \frac{1}{2} \frac{R^2}{d^2} \right) \right]}$$

$$\text{Since for } \frac{R}{d} \ll 1, \quad \sqrt{1 - \frac{R^2}{d^2}} \approx \left( 1 - \frac{1}{2} \frac{R^2}{d^2} \right)$$

$$\text{and for } d \longrightarrow \infty, \quad \frac{R^2}{d^2}, \quad \frac{\lambda^2}{4d^2} \quad \text{each} \longrightarrow 0.$$

$$(7) \quad \therefore P(\lambda) \longrightarrow \frac{\lambda}{2R^2} \quad \text{as } d \longrightarrow \infty$$

$$(8) \quad \text{And } \langle \lambda \rangle = \int_0^{2R} \lambda P(\lambda) d\lambda = \frac{1}{2R^2} \int_0^{2R} \lambda^2 d\lambda = \frac{4}{3} R$$

## APPENDIX B

### Connection between Pulse-Height Spectrum and LET Spectrum

The Proportional Counter is exposed to radiation and the number of pulses per pulse-height interval at various pulse-height intervals is measured.

Let  $N(h) dh$  = Number of pulses in the pulse-height interval  $h$  to  $h + dh$ .

Then  $N(h)$  = Number of pulses per unit pulse-height interval at the pulse-height ' $h$ '.

In the proportional counter, the pulse-height is proportional to the energy deposited within the chamber.

(1) Hence, let  $E = \alpha h$   $\alpha = \text{constant}$

Also, let  $\lambda$  and  $L$  denote respectively the path-length and the LET within the chamber.

$L$  is essentially constant within the small chamber cavity and is only a function of the energy of the incident particles.

We thus have

(2)  $E = \lambda L$

and for a constant  $L$ ,

(3)  $dE = L d\lambda$

Let  $D(L) dL$  = Number of particles with LET in the range  $L$  to  $L + dL$ .

The basic problem is to evaluate  $D(L)$  as a function of  $N(h)$  for a parallel beam of radiation incident on a proportional counter chamber of radius  $R$  cms.

The path-length distribution function for a parallel beam of radiation is given by

$$(4) \quad P(\lambda) = \frac{\lambda}{2R^2}$$

since there is a one-to-one correspondence between the number of incident particles and the number of pulses produced.

Then, the number of particles depositing energy within the cavity in the range  $E$  to  $E + dE$  per unit LET interval at the LET ' $L$ ' is,

$$(5) \quad \begin{aligned} D(E, L) dE &= D(L) P(\lambda) d\lambda \\ &= D(L) \frac{E}{2LR^2} \frac{dE}{L} \end{aligned}$$

The number of particles depositing energy within the cavity in the range  $E$  to  $E + dE$  with LET in range  $L$  to  $L + dL$  is

$$(6) \quad D(E, L) dL dE = \frac{E}{2L^2R^2} D(L) dL dE$$

Hence, the number of particles depositing energy in the cavity per unit energy interval at  $E$ , due to LET's of all values, is,

$$(7) \quad D(E) = \frac{E}{2R^2} \int_{E/2R=L_{\min}}^{\infty} \frac{D(L)}{L^2} dL$$

$$\begin{aligned} 2R^2 \frac{D(E)}{E} &= \int_{E/2R}^{\infty} \frac{D(L)}{L^2} dL \\ &= - \int_{\infty}^{E/2R} \frac{D(L)}{L^2} dL \end{aligned}$$

$$(8) \quad 2R^2 \frac{d}{dE} \left[ \frac{D(E)}{E} \right] = - \frac{d}{dE} \left[ \int_{\infty}^{E/2R} \frac{D(L)}{L^2} dL \right]$$

$$\frac{d}{dE} \left[ \int_{\infty}^{E/2R} \frac{D(L)}{L^2} dL \right] \text{ is evaluated by the following technique:}$$

$$\frac{d}{dE} \left[ f(E) \right] = \lim_{\delta E \rightarrow 0} \frac{f(E + \delta E) - f(E)}{\delta E}$$

$$\begin{aligned} \text{Hence } \frac{d}{dE} \left[ \int_{\infty}^{E/2R} \frac{D(L)}{L^2} dL \right] &= \lim_{\delta E \rightarrow 0} \frac{1}{\delta E} \left[ \int_{\infty}^{\frac{E+\delta E}{2R}} \frac{D(L)}{L^2} dL - \int_{\infty}^{E/2R} \frac{D(L)}{L^2} dL \right] \\ &= \lim_{\delta E \rightarrow 0} \frac{1}{\delta E} \left[ \int_{E/2R}^{\frac{E+\delta E}{2R}} \frac{D(L)}{L^2} dL \right] \\ &= \lim_{\delta E \rightarrow 0} \frac{1}{\delta E} \left[ \frac{D(L)}{2R L^2} \delta E \right]_{L = E/2R} \end{aligned}$$

$$(9) \quad \therefore \frac{d}{dE} \left[ \int_{\infty}^{E/2R} \frac{D(L)}{L^2} dL \right] = \frac{2R}{E^2} D(E/2R)$$

$$\text{or } 2R^2 \frac{d}{dE} \left[ \frac{D(E)}{E} \right] = - \frac{2R}{E^2} D(E/2R)$$

$$\therefore D(E/2R) = - E^2 R \frac{d}{dE} \left[ \frac{D(E)}{E} \right]$$

$$\text{Now } E = \alpha h$$

$$\frac{d}{dE} = \frac{1}{\alpha} \frac{d}{dh}$$

$$\text{and } D(E) dE = N(h) dh$$

$$= N(h) \frac{dE}{\alpha}$$

$$(10) \quad \therefore D(E) = \frac{1}{\alpha} N(h)$$

$$\begin{aligned} \text{Hence } D(E/2R) &= -\alpha^2 h^2 R \frac{1}{\alpha} \frac{d}{dh} \left[ \frac{N(h)}{\alpha^2 h} \right] \\ &= -\frac{h^2 R}{\alpha} \frac{d}{dh} \left[ \frac{N(h)}{h} \right] \end{aligned}$$

$$(11) \quad D(E/2R) = -\frac{h^2 R}{\alpha} \frac{d}{dh} \left[ \frac{N(h)}{h} \right]$$

For primary calibration, it is desired to evaluate  $D(L)$  as a function of  $N(h)$  for a radioactive source that injects into a spherical proportional counter chamber of radius  $R$  cms.

Following the same lines of argument as in the previous case, but  $P(\lambda) = 1/2R$

$$\begin{aligned} D(E, L) dE &= D(L) P(\lambda) d\lambda \\ &= D(L) \frac{1}{2R} \frac{dE}{L} \end{aligned}$$

$$(12) \quad \therefore D(E, L) dE = 2R \frac{D(L)}{L} dE$$

The number of particles depositing within the chamber energy in the range  $E$  to  $E + dE$  with LET in the range  $L$  to  $L + dL$  is

$$D(E, L) dL dE = 2R \frac{D(L)}{L} dL dE$$

Hence the number of pulses per unit energy interval at  $E$  due to LET's of all values is

$$(13) \quad D(E) = 2R \int_{E/2R}^{\infty} \frac{D(L)}{L} dL$$

$$\text{Hence } 2R \frac{d}{dE} \left[ D(E) \right] = - \frac{d}{dE} \left[ \int_{\infty}^{E/2R} \frac{D(L)}{L} dL \right]$$

$$\begin{aligned} \text{Now, } \frac{d}{dE} \int_{\infty}^{E/2R} \frac{D(L)}{L} dL &= \frac{1}{2R} \frac{D(E/2R)}{E/2R} \\ &= \frac{1}{E} D(E/2R) \end{aligned}$$

$$\begin{aligned} \therefore D(E/2R) &= - 2ER \frac{d}{dE} \left[ D(E) \right] \\ &= - 2 \propto hR \frac{1}{\propto} \frac{d}{dh} \left[ D(\propto h) \right] \end{aligned}$$

$$(14) \quad \therefore D(E/2R) = - \frac{2hR}{\propto} \frac{d}{dh} \left[ N(h) \right]$$

## APPENDIX C

### Relation of the Absorbed Dose in Rad, Q<sub>rad</sub>, to the Pulse-Height Spectrum, N(h)

For an omnidirectional flux of radiation incident on a spherical proportional counter, the LET spectrum is related to the pulse-height spectrum by the relation,

$$D(L) = D\left(\frac{E}{2R}\right) = -\frac{h^2 R}{\alpha} \frac{d}{dh} \left[ \frac{N(h)}{h} \right]$$

D(L) gives the number of particles per unit LET interval at the LET L.

The energy dissipated,  $\tilde{D}(E/2R)$ , within the chamber cavity per unit LET interval at the LET L, can be obtained from the LET distribution by multiplying D(E/2R) by the corresponding LET,  $L = E/2R$ , and by the average pathlength  $\langle \lambda \rangle = 4/3 R$ .

$$\text{Thus } \tilde{D}(E/2R) = \frac{2}{3} h^3 R \frac{d}{dh} \left[ \frac{N(h)}{h} \right]$$

and the total energy deposited within the chamber for all values of LET is,

$$\begin{aligned} \int_0^{E_{\max}} D\left(\frac{E}{2R}\right) dE &= \int_0^{h_{\max}} \frac{2\alpha}{3} L \times Rh^3 \frac{d}{dh} \left[ \frac{N(h)}{h} \right] dh \\ &= \frac{2\alpha R}{3} \int_0^{h_{\max}} h^3 \frac{d}{dh} \left[ \frac{N(h)}{h} \right] dh \\ &= \frac{2\alpha R}{3} \left[ h^2 N(h) \Big|_0^{h_{\max}} - \int_0^{h_{\max}} 3h N(h) dh \right] \\ &= \frac{2\alpha R}{3} \left[ h^2 N(h) \Big|_0^{h_{\max}} - 3 \int_0^{h_{\max}} h N(h) dh \right] \end{aligned}$$

The energy in units of rad is obtained as,

$$Q_{\text{rad}} = \frac{2 \alpha R}{300 P_{\text{gas}} V} \left[ h^2 N(h) \Big|_0^{h_{\text{max}}} - 3 \int_0^{h_{\text{max}}} h N(h) dh \right]$$

where  $P_{\text{gas}}$  = Density of gas in chamber

$V$  = Volume of chamber cavity.

## APPENDIX D

### Bragg-Gray Theory

If a measurement of the radiation energy absorbed in a given material is desired, the Bragg-Gray relation may be used.

$$E = SWJ$$

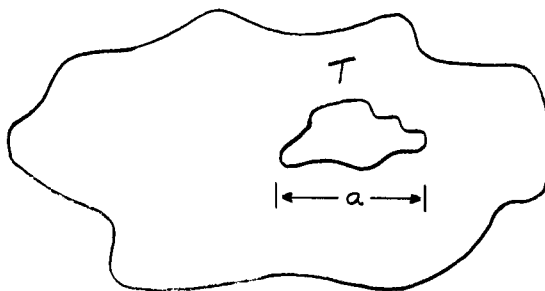
where  $E$  = energy absorbed per gm per sec by the material irradiated

$S$  = electronic mass stopping power of the solid material irradiated relative to the gas in a small cavity in the irradiated material

$W$  = energy required to produce an ion pair in the cavity gas

$J$  = ion current in ion pairs per gm per sec of gas in the cavity.

This principle may be derived in many ways. A straightforward approach is as follows. Let a block of material be irradiated with gamma rays. A flux of secondary electrons  $M(E)$  from pair production, Compton, and photoelectric electrons will be produced. In the interior of this piece of material, consider a small region  $T$  with a certain linear dimension  $a$ .



The energy lost by an electron crossing this region will then be  $(a)(dE/dx)$ . The energy lost per second by the entire spectrum is

$$E_{\text{solid}} = \int M(E, \theta) a(\theta) \left( \frac{dE}{dx} \right)_{\text{solid}} d\theta dE$$

Make T small enough so that its removal will not change M(E). If the solid material in the region is now removed, and the resulting cavity filled with a gas, the energy lost per second in the gas is

$$E_{\text{gas}} = \int M(E, \theta) a(\theta) \left( \frac{dE}{dx} \right)_{\text{gas}} d\theta dE$$

The ratio of the two integrals is the relative stopping power S.

$$\frac{\left\langle \frac{dE}{dx} \right\rangle_{\text{solid}}}{\left\langle \frac{dE}{dx} \right\rangle_{\text{gas}}} = \frac{E_{\text{solid}}}{E_{\text{gas}}}$$

or  $E_{\text{solid}} = S E_{\text{gas}}$

The energy per cubic centimeter of gas may be written as

$$E_{\text{gas}} = WJ$$

where W is the energy to produce an ion pair in the gas, and J is the ion current in ion pairs per cubic centimeter per second. Combining the above two equations gives the Bragg-Gray principle

$$E_{\text{solid}} = SWJ_{\text{gas}}$$

An alternate method of writing is

$$E_M = S_M W J_M$$

where  $E_M$  = energy absorption of ev/gm sec

$S_M$  = mass stopping power of the wall material relative to the cavity gas

$J_M$  = ion current in ion pairs per gm per second.